IEEE Access
Multidisciplinary ⋮ Rapid Review ⋮ Open Access Journal

Received July 25, 2020, accepted August 4, 2020, date of publication August 17, 2020, date of current version August 27, 2020.

Digital Object Identifier 10.1109/ACCESS.2020.3016975

Time Domain Simplified Equations and Its Iterative Calculation Model for LLC Resonant Converter

JINGKAI NIU[1], (Graduate Student Member, IEEE), YIBING TONG[1], QING DING[2], XUEZHI WU[1], XIAOMIN XIN[1], AND XIN WANG[1]

[1]School of Electrical Engineering, Beijing Jiaotong University, Beijing 100044, China
[2]Shenzhen Power Supply Bureau Company Ltd., Shenzhen 518000, China

Corresponding author: Yibing Tong (ybtong@bjtu.edu.cn)

This work was supported in part by National Key Research and Development Program of China under Grant 2018YFB0905305, and in part by Project of Science and Technology China Southern Grid under Grant 090000KK52190002.

ABSTRACT LLC resonant converters can achieve soft switching and loss reduction. However, the analysis methods of wide frequency range LLC converters generally have problems with incomplete working condition analysis at non-resonant frequencies and there is always a tradeoff between the accuracy and the simplicity. These problems will affect the loss calculation, synchronous rectification and so on. The research objective of this paper focuses on the full-bridge LLC resonant converter. In this paper, three conditions are analyzed in time-domain including switching frequency lower than the resonant frequency at heavy load, switching frequency lower than the resonant frequency at light load, and switching frequency larger than the resonant frequency. Based on proper assumption and simplification, the approximate equivalent of the trigonometric function is used to simplify the complex time-domain equations. The simplified equations are obtained with the resonant capacitor voltage and resonant inductor current as the key variables. In order to make the simplified equations easy to use, an iterative calculation model is proposed with more simplicity than sophisticated software to solve nonlinear equations. The simplified equations and the model proposed in this paper are verified by comparison with the fundamental analysis methods, the simulation, and the experiments. By using the iterative calculation model, the voltage, current, time and other variables of switching points can be obtained with the relative error less than 3% to theoretic values, which can be used in loss calculation, synchronous rectification and so on. And the iterative calculation model can be realized on DSP or other processors in real-time.

INDEX TERMS LLC resonant converter, time domain, simplified equations, and iterative calculation.

I. INTRODUCTION

In recent years, LLC resonant converters have been widely applied in photovoltaic, electric vehicles and other fields because of their characteristics of soft switching in the full load range, and are developing towards high frequency, high efficiency and high power density with the help of wide band-gap devices [1]–[4].

Different from other DC-DC converters like Buck, Boost and so on, the analysis of resonant converter cannot be carried out by the state-space average method. Several analysis methods have been developed in the past. They can be summarized into three categories: 1) fundamental harmonic approximation (FHA), 2) FHA with time-domain corrections and 3) time domain analysis (TDA).

FHA method is the most widely used because that it is easier to obtain the converter's voltage gain and the switching frequency range by concise mathematical formulas [5]–[7]. However, because FHA method is a kind of frequency domain method and assumes that only the fundamental component of primary square voltage transfers energy to load, which is not very accurate since the fact is that high harmonic components also transfer energy to load. Especially, when the switching frequency is far away from the resonant frequency, the resonant current has a serious distortion. On the other hand, some electric parameters used

The associate editor coordinating the review of this manuscript and approving it for publication was Zhe Zhang.

to design LLC converters cannot be accurately analyzed by FHA method, such as the peak resonant current used to design the resonant inductor, the peak magnetizing current used to design the transformer, the resonant current RMS value used for the loss calculation and so on.

In order to improve the analysis accuracy, many studies have been conducted to analyze the characteristics of the converter based on time domain method in recent years. In the literature [8], combining with TDA method and FHA method, a novel over-current protection circuit for LLC converter is proposed. But most of the analysis is on the basis of FHA such as the primary current RMS value expression and the voltage gain expression. So the analysis error is large. In the literature [9], the voltage gain and the equivalent load under discontinuous conduction mode are modified by using the time-domain analysis. For this method, although the accuracy of this method is slightly improved compared with FHA, it still makes many assumptions, which will decrease its accuracy compared with the practical results. For example, the authors believe that the secondary current is sinusoidal, which contradicts the fact that the primary resonant current is not sinusoidal, especially in a wide output voltage range. In the literature [10], the converter gain expression is redefined by combining time domain and frequency domain, and resonant factor and load factor are analyzed. But the definition of resonant factor and load factor is based on insufficient basis and lacks the experimental verification. The derivation procedure is complicated and the accuracy improvement is not obvious. In the literature [11], [12], time domain methods are used to find out all the possible parameters that can satisfy the required peak gain in PN and PON modes. However, the soft-switching condition of the converter will be lost and the switching losses will be increased. Besides, all the design results are just satisfied with the peak gain requirement, but the conditions at full frequency range are not discussed. In the literature [13], a voltage-fed full-bridge LLC resonant converter with symmetrical quadrupler rectifier circuit is analyzed with TDA method. But the equations are complex and need further simplification. In the literature [14], [15], the time-domain equations are simplified which make the conduction angles of the synchronous rectifiers easier to calculate. But some improper assumptions are used in the simplification. For example, the authors think the resonant current remain unchanged during the period while the LLC converter's rectifier is in the off-state, which only applies if the excitation inductor is much larger than the resonant inductor. In the literature [16], a new average small-signal modeling technique is proposed based on [14], [15], so the unsuitable assumptions still exist. In the literature [17]–[19], the power loss estimation methods are presented with TDA method. But the equations to be solved contains a large number of unknowns and the difficulty of solving the equations is not considered. In the literature [20], the TDA is used to analyze the LLC resonant converter in DCM boost mode, and the formulas of voltage gain and current effective value are given. But no detailed analysis has been made on the working condition that the switching frequency is larger than the resonance frequency. In the literature [21], the TDA is used to optimize the efficiency of LLC resonant converters and the equations composed of related variables are given. But the solution process for the equations is not mentioned.

It can be summarized from the above literatures that the TDA method has higher accuracy than FHA method and can be used to analyze the loss, the design of the magnetic components and synchronous rectification, etc. Without the assumptions and simplification, the time-domain equations contain a large number of trigonometric functions and unknowns which are difficult to deal with. So most TDA methods make assumptions and make simplifications based on these assumptions. However, some of the assumptions are wrong or only suitable for specific occasions and some of the simplifications are of small significance.

In order to make more suitable assumptions, this paper analyzes the full bridge LLC resonant converter under three typical working conditions, which are divided based on the switching frequency and load, in time-domain, and the time-domain functions of each time period are obtained. According to the characteristics of each time period, the assumptions are made so that many triangle functions that are difficult to deal with in time domain analysis can be approximated. These assumptions do not seriously violate the actual waveform shape and physical characteristics, and verified by using the actual parameters in the reference.

Based on above assumptions, simplifications are made from the following two perspectives: 1) using the relation of inductance, capacitance, time and impedance to simplify, 2) making the resonant capacitor voltage and the resonant inductor current of the switching points as key variables which can be used to obtain the complete time-domain function and analyze the loss, the design of the magnetic components and so on. A simplified set of equations with the resonant capacitor voltage and the resonant inductor current as key variables is obtained after the simplifications.

In order to solve the simplified time domain equations without sophisticated software to solve nonlinear equations, an iterative calculation model is proposed. All variables are divided into two groups. The iterative solution formula between two groups of variables is obtained by simultaneous multiple equations. The suitable initial solution is proposed to put into the iterative formula, then all variables are solved with the relative error less than 3% to theoretic values, which can be used in loss calculation, synchronous rectification and so on.

This paper is organized as follows. Time domain analysis of the full-bridge LLC resonant converter under three typical working conditions, the assumptions and simplifications are analyzed in Section II. In Section III, the iterative calculation model is proposed. In Section IV, some experimental and simulation results are presented to verify the simplified time domain equations and the iterative calculation model. In Section V, some conclusions about the simplified time

domain equations and the iterative calculation model are summarized.

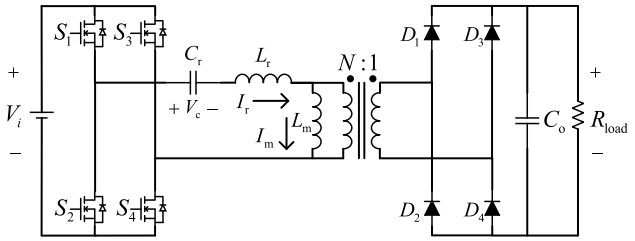

FIGURE 1. Full-bridge LLC resonant converter topology.

II. SIMPLIFIED TIME DOMAIN EQUATIONS

The topology of full bridge LLC resonant converter is shown in Fig. 1.

Where S_1–S_4 are active switches, D_1–D_4 are diodes, L_r is the resonant inductor, C_r is the resonant capacitor, L_m is the excitation inductance of primary side of the transformer, turn ratio of transformer is N:1, C_o is the output filter capacitor, R_{load} is the load resistance. The switching frequency of the primary switches is f_s. The voltage of C_r is V_c, the current of L_r is I_r, the excitation current is I_m, the input voltage is V_i, the output voltage is V_o and the output current is I_o. The reference direction is shown in Fig. 1.

The resonant frequency f_r, the normalized switching frequency f_n, the angular velocity ω_r and ω_m, the inductance coefficient L_n, the resonance impedance Z_r, the voltage V_o^* and the current I_o^* are defined as:

$$f_r = \frac{1}{2\pi\sqrt{L_r C_r}} \tag{1.1}$$

$$f_n = \frac{f_s}{f_r} \tag{1.2}$$

$$\omega_r = \frac{1}{\sqrt{L_r C_r}} \tag{1.3}$$

$$\omega_m = \frac{1}{\sqrt{(L_r + L_m)C_r}} \tag{1.4}$$

$$L_n = \frac{L_m}{L_r} \tag{1.5}$$

$$Z_r = \sqrt{\frac{L_r}{C_r}} \tag{1.6}$$

$$V_o^* = NV_o \tag{1.7}$$

$$I_o^* = \frac{I_o}{N} \tag{1.8}$$

In order to simplify the analysis, the influence of dead time and other stray parameters are not considered. When the primary leakage inductor cannot be ignored, it should be regarded as a part of L_r. At the same time, it is assumed that C_o is large enough, and V_o will not change in the steady-state.

Under different working conditions, the equivalent circuit of LLC resonant circuit varies in different periods, and the load has little influence on the condition when the switching frequency is greater than the resonant frequency. Therefore, three working conditions are analyzed in this paper, including Condition I: $f_n < 1$ with heavy load; Condition II: $f_n < 1$ with light load; Condition III: $f_n > 1$.

The waveforms of the resonant inductance current i_r, the excitation current i_m, the resonant capacitance voltage v_c and the primary winding voltage v_t under three working conditions are shown in Fig. 2. 0, t_1, t_2 and t_3 are the time when the switch states of the LLC resonant converter change. In these moments, the resonant inductance currents and the resonant capacitance voltage are defined as I_{r0}, I_{r1}, I_{r2}, I_{r3}, V_{c0}, V_{c1}, V_{c2} and V_{c3}.

A. SIMPLIFICATION OF CONDITION I

Referring to the known time-domain analysis [20], the time-domain functions of each time period under Condition I can be obtained:

0–t_1:

$$\begin{cases} v_c(t) = I_{r0}Z_r \sin(\omega_r t) + (V_{c0} - V_i + V_o^*)\cos(\omega_r t) \\ \qquad +V_i - V_o^* \\ i_r(t) = I_{r0}\cos(\omega_r t) - \dfrac{V_{c0} - V_i + V_o^*}{Z_r}\sin(\omega_r t) \\ i_m(t) = I_{r0} + \dfrac{V_o^*}{L_m}t \end{cases} \tag{1.9}$$

t_1–t_2:

$$\begin{cases} v_c(t) = I_{r1}\sqrt{(L_n+1)}Z_r \sin(\omega_m t - \omega_m t_1) \\ \qquad +(V_{c1} - V_i)\cos(\omega_m t - \omega_m t_1) + V_i \\ i_r(t) = I_{r1}\cos(\omega_m t - \omega_m t_1) - \dfrac{V_{c1} - V_i}{\sqrt{(L_n+1)}Z_r} \\ \qquad \times \sin(\omega_m t - \omega_m t_1) \\ i_m(t) = i_r(t) \end{cases} \tag{1.10}$$

t_1 and t_2 are defined as follows:

$$\begin{cases} t_1 = \dfrac{T_k T_r}{2} \\ t_2 = \dfrac{T_n T_r}{2} \end{cases} \tag{1.11}$$

where T_r is L_rC_r resonant period, T_k is the time coefficient to be calculated and T_n are defined as:

$$T_n = \frac{1}{f_n} \tag{1.12}$$

In most conditions, L_m is larger than L_r, ω_m is smaller than ω_r and the time period from t_1 to t_2 is short. So the change of i_r is very small in this period and the time period from 0 to t_1 can be regarded as $T_r/2$ in [10], [16]. But the requirements "$I_{r0} + I_{r1} = 0$" and "$V_{c0} + V_{c1} = 0$" are only met when f_s is equal to f_r. This means t_1 is not equal to $T_r/2$. So T_k is introduced to describe the relationship between t_1 and $T_r/2$. And T_k is approx. equal to 1 in most conditions.

For the approximations of the time-domain functions in 0–t_1, due to $T_k \approx 1$ and $\omega_r t_1 \approx \pi$, the following approximation can be obtained.

$$\begin{cases} \sin(\omega_r t_1) \approx \pi(1 - T_k) \\ \cos(\omega_r t_1) \approx -1 \end{cases} \tag{1.13}$$

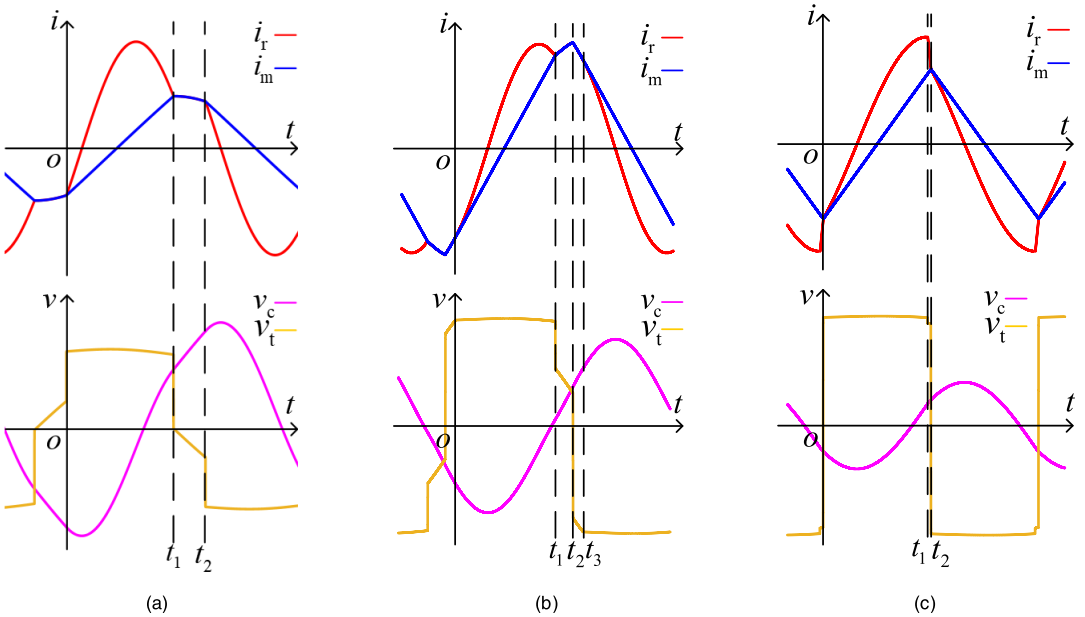

FIGURE 2. Related waveforms of resonant converter under: (a) Condition I; (b) Condition II; (c) Condition III, where i_r: the resonant inductance current; i_m: the excitation current; v_c: the resonant capacitance voltage; v_t: the primary winding voltage.

By combining $t = t_1$, (1.9), (1.11) and (1.13), the following equation can be obtained.

$$\pi(T_k - 1) \times I_{r0}Z_r + (V_{c0} + V_{c1}) = 2 \times (V_i - V_o^*) \quad (1.14)$$

$$(I_{r0}Z_r + I_{r1}Z_r) = -\pi(T_k - 1) \times (V_i - V_o^* - V_{c0}) \quad (1.15)$$

$$-I_{r0}Z_r + I_{r1}Z_r = \frac{\pi}{L_n} T_k V_o^* \quad (1.16)$$

For the approximations of the time-domain functions in t_1–t_2, due to $\omega_m t_2 - \omega_m t_1 \approx 0$, the following approximation can be obtained.

$$\begin{cases} \sin(\omega_m t_2 - \omega_m t_1) \approx \omega_m t_2 - \omega_m t_1 \\ \cos(\omega_m t_2 - \omega_m t_1) \approx 1 \end{cases} \quad (1.17)$$

In order to verify the validity of the approximation, $\omega_m t_2 - \omega_m t_1$ can be transformed as follow.

$$\omega_m t_2 - \omega_m t_1 \approx \frac{\pi(\frac{1}{f_n} - 1)}{\sqrt{(L_n + 1)}} \quad (1.18)$$

The data in several papers are cited to calculate the approximate scope of $\omega_m t_2 - \omega_m t_1$. The results are shown in the table below.

From the table above, it can be seen that the requirement "$\omega_m t_2 - \omega_m t_1 < 0.5$" is generally met. The larger the value of $\omega_m t_2 - \omega_m t_1$ is, the larger the approximate error will be. When the requirement of "$\omega_m t_2 - \omega_m t_1 = 0.5$" is met, the approximate error can be calculated as shown below.

$$\left| \frac{\cos(\omega_m t_2 - \omega_m t_1) - 1}{\cos(\omega_m t_2 - \omega_m t_1)} \right| \approx 0.14 \quad (1.19)$$

$$\left| \frac{\sin(\omega_m t_2 - \omega_m t_1) - (\omega_m t_2 - \omega_m t_1)}{\sin(\omega_m t_2 - \omega_m t_1)} \right| \approx 0.04 \quad (1.20)$$

When the requirement of " $\omega_m t_2 - \omega_m t_1$ <0.5" is met, the approximate error of sine function is small enough to be acceptable. But the approximate error of cosine function is still large, which means further correction is still needed.

TABLE 1. Related parameters in other papers.

Minimum value of f_n	L_n	$\omega_m t_2 - \omega_m t_1$
150k/200k=0.75[8]	3.4	0.4992
3k/5k=0.6[10]	20	0.4570
230k/270k=0.8519[13]	14.28	0.1397
71.43k/93k=0.7681[15]	9.6	0.2913
75k/96k=0.7813[16]	2.9268	0.4438
150k/189k=0.7937[18]	2.7427	0.4221
480k/670k=0.7164[21]	7	0.4397

By combining (1.10) and (1.17), the following equations can be obtained.

$$\begin{cases} v_c(t) = \frac{I_{r1}}{C_r}(t - t_1) + V_{c1} \\ i_r(t) = I_{r1} - \frac{V_{c1} - V_i}{(L_n + 1)L_r}(t - t_1) \end{cases} \quad (1.21)$$

It can be seen from (1.21) that I_{r1} determines the change rate of the resonant capacitor voltage and is a constant, but in fact, the change rate is affected by the resonant inductor current and is not a constant. This contradiction is caused by the approximate error. In order to solve this contradiction, the equivalent current is introduced to replace I_{r1} in the expression of the resonant capacitor voltage. In the period from t_1 to t_2, the resonant inductor current keeps changing and the change is nearly linear. So the average value of the resonant inductor current in this period can be regard as the equivalent current and can be expressed as $(I_{r1} + I_{r1})/2$. Similarly, the equivalent voltage expressed as $(V_{c1} + V_{c2})/2$ is introduced to

replace V_{c1} in the expression of the resonant inductor voltage. After the above correction, the equations of the period from t_1 to t_2 can be obtained as follow.

$$\begin{cases} V_{c2} = \dfrac{I_{r1}+I_{r2}}{2C_r}(t_2-t_1)+V_{c1} \\ I_{r2} = I_{r1} - \dfrac{V_{c1}+V_{c2}-2V_i}{2(L_n+1)L_r}(t_2-t_1) \end{cases} \tag{1.22}$$

When the requirement of "$\omega_m t_2 - \omega_m t_1 > 0.5$" is met, the approximate errors of sine and cosine functions are both large even when the corrections are made. This will converge to inaccurate or even wrong results when using the following iterative algorithm. Therefore, it is not recommended to use these simplified equations when f_s is far lower than f_r or L_n is too small. In fact, a very wide frequency range will make it difficult to design magnetic components. And more and more LLC designs use transformer leakage inductance as resonance inductance, which means a large L_n. In other words, the assumptions about the approximation and the correction made in this paper are applicable to some extent.

The following equations can be seen from the symmetry of resonance waveform:

$$\begin{cases} V_{c2} = -V_{c0} \\ I_{r2} = -I_{r0} \end{cases} \tag{1.23}$$

By combining (1.11), (1.22) and (1.23), the following equation can be obtained.

$$-\frac{\pi}{2}(T_n - T_k) \times (I_{r0}Z_r - I_{r1}Z_r) + (V_{c0} + V_{c1}) = 0 \tag{1.24}$$

$$\frac{2}{\pi}(L_n+1) \times (I_{r0}Z_r + I_{r1}Z_r) = -(T_n - T_k) \times (2V_i + V_{c0} - V_{c1}) \tag{1.25}$$

From the perspective of energy transfer, the following equation is also considered.

$$\int_0^{t_2} (i_r - i_m)dt = \int_0^{t_2} I_o^* dt \tag{1.26}$$

Using (1.9) and (1.10) to simplify (1.26), we can get:

$$-T_k \times (I_{r0}Z_r + I_{r1}Z_r) - \frac{2}{\pi} \times (V_{c0} - V_{c1}) = 2T_n \times I_o^* Z_r \tag{1.27}$$

The simplified time-domain equation for Condition I is as follows.

$$\begin{cases} \pi(T_k - 1) \times I_{r0}Z_r + (V_{c0} + V_{c1}) = 2 \times (V_i - V_o^*) \\ (I_{r0}Z_r + I_{r1}Z_r) = -\pi(T_k - 1) \times (V_i - V_o^* - V_{c0}) \\ -(I_{r0}Z_r - I_{r1}Z_r) = \dfrac{\pi}{L_n} T_k \times V_o^* \\ -\dfrac{\pi}{2}(T_n - T_k) \times (I_{r0}Z_r - I_{r1}Z_r) + (V_{c0} + V_{c1}) = 0 \\ \dfrac{2}{\pi}(L_n+1) \times (I_{r0}Z_r + I_{r1}Z_r) \\ \quad = -(T_n - T_k) \times (2V_i + V_{c0} - V_{c1}) \\ -T_k \times (I_{r0}Z_r + I_{r1}Z_r) - \dfrac{2}{\pi} \times (V_{c0} - V_{c1}) = 2T_n \\ \quad \times I_o^* Z_r \end{cases} \tag{1.28}$$

In order to clarify the relationship between variables, the matrix of equations can be obtained as follow by transforming (1.28). Eq. (1.29), as shown at the bottom of the next page.

By comparing with the equations solved in other papers, equations we proposed in this manuscript are simpler. From the matrix form of the equation shown below, it is noted that the parts at both ends of the equal sign are the product of a coefficient matrix and a voltage matrix without variables related to time and frequency. T_k and T_n are coefficients without units. Therefore when the resonance frequency changes, as long as V_i, V_o^*, I_o^*, Z_r and L_n are the same, the shapes of voltage and current waveforms remain the same as well as V_{c0}, V_{c1}, I_{r0} and I_{r1}. This characteristic also exists in FHA method, which has never been mentioned in other existing TDA papers.

B. SIMPLIFICATION OF CONDITION II

The analysis in 0–t_2 under Condition II is the same as that under Condition I. In t_2–t_3, the primary winding voltage is too low to make rectifier diodes on secondary side conduct. The circuit state and equivalent circuit in this period are shown in Fig. 3 and Fig. 4.

From the above analysis, it can be seen that there is the following equation at t_3:

$$(V_{c3} + V_i)\frac{L_m}{L_r + L_m} = V_o^* \tag{1.30}$$

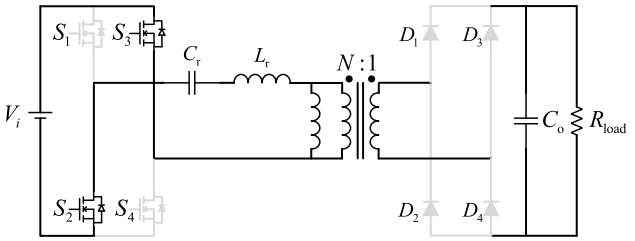

FIGURE 3. The circuit state in $t_2 - t_3$ under Condition II.

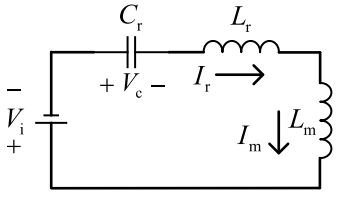

FIGURE 4. The equivalent circuit in $t_2 - t_3$ under Condition II.

Similar to the time-domain analysis in [20], the time-domain functions in t_2–t_3 under Condition I can be obtained:

$$\begin{cases} v_c(t) = I_{r2}\sqrt{(L_n+1)}Z_r \sin(\omega_m t - \omega_m t_2) \\ \qquad +(V_{c2}+V_i)\cos(\omega_m t - \omega_m t_2) - V_i \\ i_r(t) = I_{r2}\cos(\omega_m t - \omega_m t_2) \\ \qquad -\dfrac{V_{c2}+V_i}{\sqrt{(L_n+1)}Z_r}\sin(\omega_m t - \omega_m t_2) \\ i_m(t) = I_{r2}\cos(\omega_m t - \omega_m t_2) \\ \qquad -\dfrac{V_{c2}+V_i}{\sqrt{(L_n+1)}Z_r}\sin(\omega_m t - \omega_m t_2) \end{cases} \tag{1.31}$$

Define t_1, t_2 and t_3 as follows. Similar to T_k, T_d is introduced to describe the relationship between t_2 and $T_s/2$. The time period from t_2 to t_3 is usually short, so $T_d \approx 1$.

$$\begin{cases} t_1 = \dfrac{T_k T_r}{2} \\ t_2 = \dfrac{T_d T_n T_r}{2} \\ t_3 = \dfrac{T_n T_r}{2} \end{cases} \tag{1.32}$$

Similar to (1.17) and (1.22), the approximation and the correction are applied to (1.31). For details, please see the Appendix B. The simplified time-domain equations of Condition II are given as (1.33), as shown at the bottom of the page.

C. SIMPLIFICATION OF CONDITION III

The analysis in 0–t_1 under Condition III is the same as that under Condition I. At time t_1, the states of switches change. In t_1–t_2, the circuit state and equivalent circuit under Condition III are shown in Fig. 5 and Fig. 6.

Define t_1 and t_2 as (1.11).

It can be seen from Fig. 6 that V_i and V_o^* act on L_r and C_r together, which makes the resonant current decrease rapidly, so the time period of t_1–t_2 is generally very short and T_k is approximately equal to T_n.

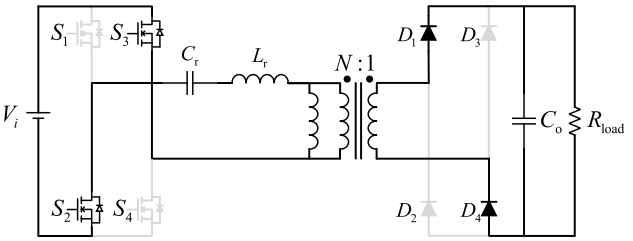

FIGURE 5. The circuit state in $t_1 - t_2$ under Condition III.

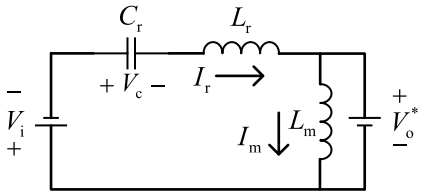

FIGURE 6. The equivalent circuit in $t_1 - t_2$ under Condition III.

The approximation of (1.17) and the correction of (1.22) are unable to meet the needs under Condition III. The following equations are obtained after $t = t_1$ and (1.11) are plugged

$$\begin{bmatrix} \pi(T_k-1) & 0 & 1 & 1 \\ 1 & 1 & -\pi(T_k-1) & 0 \\ -1 & 1 & 0 & 0 \\ -\dfrac{\pi}{2}(T_n-T_k) & \dfrac{\pi}{2}(T_n-T_k) & 1 & 1 \\ \dfrac{2}{\pi}(L_n+1) & \dfrac{2}{\pi}(L_n+1) & (T_n-T_k) & -(T_n-T_k) \\ -T_k & -T_k & -\dfrac{2}{\pi} & \dfrac{2}{\pi} \end{bmatrix} \begin{bmatrix} I_{r0}Z_r \\ I_{r1}Z_r \\ V_{c0} \\ V_{c1} \end{bmatrix} = \begin{bmatrix} 2 & -2 & 0 \\ -\pi(T_k-1) & \pi(T_k-1) & 0 \\ 0 & \dfrac{\pi}{L_n}T_k & 0 \\ 0 & 0 & 0 \\ -2(T_n-T_k) & 0 & 0 \\ 0 & 0 & 2T_n \end{bmatrix} \begin{bmatrix} V_i \\ V_o^* \\ I_o^* Z_r \end{bmatrix} \tag{1.29}$$

$$\begin{bmatrix} \pi(T_k-1) & 0 & 0 & 1 & 1 & 0 \\ 1 & 1 & 0 & -\pi(T_k-1) & 0 & 0 \\ -1 & 1 & 0 & 0 & 0 & 0 \\ 0 & \frac{\pi}{2}(T_k-T_dT_n) & \frac{\pi}{2}(T_k-T_dT_n) & 0 & -1 & 1 \\ 0 & \frac{2}{\pi}(L_n+1) & -\frac{2}{\pi}(L_n+1) & 0 & (T_k-T_dT_n) & (T_k-T_dT_n) \\ -T_k & -T_k & 0 & -\frac{2}{\pi} & \frac{2}{\pi} & 0 \\ \frac{\pi}{2}T_n(1-T_d) & 0 & -\frac{\pi}{2}T_n(1-T_d) & -1 & 0 & -1 \\ \frac{2}{\pi}(L_n+1) & 0 & \frac{2}{\pi}(L_n+1) & T_n(1-T_d) & 0 & -T_n(1-T_d) \\ 0 & 0 & 0 & 1 & 0 & 0 \end{bmatrix} \begin{bmatrix} I_{r0}Z_r \\ I_{r1}Z_r \\ I_{r2}Z_r \\ V_{c0} \\ V_{c1} \\ V_{c2} \end{bmatrix}$$

$$= \begin{bmatrix} 2 & -2 & 0 \\ -\pi(T_k-1) & \pi(T_k-1) & 0 \\ 0 & \frac{\pi}{L_n}T_k & 0 \\ 0 & 0 & 0 \\ 2(T_k-T_dT_n) & 0 & 0 \\ 0 & 0 & 2T_n \\ 0 & 0 & 0 \\ 2T_n(1-T_d) & 0 & 0 \\ 1 & -(\frac{1}{L_n}+1) & 0 \end{bmatrix} \begin{bmatrix} V_i \\ V_o^* \\ I_o^* Z_r \end{bmatrix} \tag{1.33}$$

into (1.9).

$$\begin{cases} V_{c1} - V_i + V_o^* = I_{r0}Z_r \sin(\pi T_k) + (V_{c0} - V_i \\ \qquad +V_o^*)\cos(\pi T_k) \\ I_{r1}Z_r = I_{r0}Z_r \cos(\pi T_k) - (V_{c0} - V_i + V_o^*)\sin(\pi T_k) \end{cases} \tag{1.34}$$

Using the analysis method of SOTC for reference [22], (1.30) can be reduced to the following equations:

$$\left(V_{c0}-V_i+V_o^*\right)^2+(I_{r0}Z_r)^2=\left(V_{c1}-V_i+V_o^*\right)^2+(I_{r1}Z_r)^2 \tag{1.35}$$

$$\tan(\pi T_k)=\frac{\left(V_{c1}-V_i+V_o^*\right)I_{r0}Z_r-\left(V_{c0}-V_i+V_o^*\right)I_{r1}Z_r}{I_{r0}I_{r1}Z_r^2+\left(V_{c1}-V_i+V_o^*\right)\left(V_{c0}-V_i+V_o^*\right)} \tag{1.36}$$

Equation (1.31) can be simplified as follows:

$$(V_{c0}-V_{c1})\left(V_{c0}+V_{c1}-2V_i+2V_o^*\right)=(I_{r1}-I_{r0})\left(I_{r1}+I_{r0}\right)Z_r^2 \tag{1.37}$$

In general, considering the design of the magnetic components and the loss of the primary side switch, the switching frequency will not be more than twice of the resonance frequency and $0.5 < T_n < 1$. Due to the relationship of $T_k \approx T_n$, $0.5\pi < \pi T_k < \pi$ is usually satisfied under Condition III, namely, $|\pi(1 - T_k)| < 0.5\pi$. Then Taylor expansion can be used as follow.

$$\tan(x) = \sum_{n=1}^{\infty} \frac{(-1)^{n-1}\,2^{2n}\left(2^{2n}-1\right)B_{2n}}{(2n)!}x^{2n-1},\ |x| < \frac{\pi}{2} \tag{1.38}$$

where B_{2n} is the 2n term of Bernoulli number. According to the requirement of precision, $\tan(x)$ can be expanded by selecting the appropriate items. If two terms are taken here for expansion, the following equation can be obtained:

$$-\tan(\pi T_k) \approx \pi(1 - T_k) + \frac{\pi^3}{3}(1 - T_k)^3 \tag{1.39}$$

Due to the relationship of $T_k \approx T_n$, when $f_r < f_s < 1.275f_r$, the approximate relative error of (1.39) is less than 3% because $0.784 < T_k < 1$. If the switching frequency is too high to meet the above conditions, more items shall be taken for expansion to ensure the calculation accuracy.

By combining (1.36) and (1.39), the univariate third-order lacunary equation can be obtained with T_k as the unknown number. According to the practical significance, the effective solution is real solution, then the Cardano's Formula can be used to solve it, as follows:

$$X = \frac{\left(V_{c1} - V_i + V_o^*\right)I_{r0}Z_r - \left(V_{c0} - V_i + V_o^*\right)I_{r1}Z_r}{I_{r0}I_{r1}Z_r^2 + \left(V_{c1} - V_i + V_o^*\right)\left(V_{c0} - V_i + V_o^*\right)} \tag{1.40}$$

$$T_k = 1+\frac{1}{\pi}\left(\sqrt[3]{\frac{3X}{2}+\sqrt{\frac{9X^2}{4}+1}}+\sqrt[3]{\frac{3X}{2}-\sqrt{\frac{9X^2}{4}+1}}\right) \tag{1.41}$$

Equations (1.40) and (1.41) are parts of the simplified time-domain equation. Similar to Condition I and Condition II, the approximation and the correction are applied to the period t_1–t_2 of Condition III. Details are shown in the Appendix C. The rest parts of the simplified time-domain equations of Condition III are given as follows.

$$\begin{bmatrix} \frac{\pi}{2}(T_k - T_n) & -\frac{\pi}{2}(T_k - T_n) & 1 & 1 \\ \frac{2}{\pi} & \frac{2}{\pi} & (T_n - T_k) & -(T_n - T_k) \\ 1 & 0 & 0 & 0 \\ 0 & 0 & -1 & 0 \end{bmatrix} \times \begin{bmatrix} I_{r0}Z_r \\ I_{r1}Z_r \\ V_{c0} \\ V_{c1} \end{bmatrix} = \begin{bmatrix} 0 & 0 & 0 \\ 2(T_n - T_k) & 2(T_n - T_k) & 0 \\ 0 & -\frac{T_n}{2L_n} & 0 \\ 0 & 0 & \frac{\pi}{2}T_n \end{bmatrix} \begin{bmatrix} V_i \\ V_o^* \\ I_o^*Z_r \end{bmatrix} \tag{1.42}$$

III. ITERATIVE CALCULATION MODEL

Three sets of simplified time-domain equations are obtained. All variables can be calculated by solving these equations so that all waveforms of LLC resonant converter can be reproduced. But the accurate expressions of variables are difficult to derive. The traditional numerical methods need large amount of calculation cost and are difficult to realize on the microprocessors in real-time.

In this paper, an iterative algorithm is designed to improve the practicability of the simplified time-domain equations and can be realized on DSP or other processors in real time.

The basic idea of the iterative algorithm proposed in this paper is as follows:

1) The variables to be solved are divided into two groups: one is the time coefficients, including T_n, T_k and T_d; the other is the key variables related to voltage and current, including V_{c0}, V_{c1}, V_{c2}, I_{r0}, I_{r1} and I_{r2}.

2) The equations under the same working condition are simplified and divided into two sets of solutions: the solutions for T_n, T_k and T_d which are expressed by V_i, V_o^*, I_o^*, Z_r, L_n, V_{c0}, V_{c1}, V_{c2}, I_{r0}, I_{r1} and I_{r2}; the solutions for V_{c0}, V_{c1}, V_{c2}, I_{r0}, I_{r1} and I_{r2} which are expressed by V_i, V_o^*, I_o^*, Z_r, L_n, T_n, T_k and T_d.

3) Considering the approximate value of T_n, T_k and T_d, a set of suitable values can be taken as the initial value for the iterative calculation.

4) When the errors of the last two groups of iterative variables are large, the iteration is continued until the accuracy requirements are met, and the final solutions are obtained.

The simplification process of the three working conditions is complex, and the derivation process is shown in the Appendix A. The iterative formulas of Condition I is as

follows in (2.1), as shown at the bottom of the page, where (i) and (i+1) are iterative numbers.

Due to $T_k \approx 1$, by combining $T_{k(0)} = 1$ and (2.2), as shown at the bottom of the page, the initial value under Condition I can be obtained as follows:

$$\begin{cases} T_{k(0)} = 1 \\ T_{n(0)} = 1 + \dfrac{4L_n}{\pi^2}(1 - \dfrac{V_i}{V_o^*}) \end{cases} \tag{2.3}$$

After simplification of the equations under Condition II, it can be seen that two variables are fixed values:

$$\begin{cases} V_{c0} = V_i - (\dfrac{1}{L_n} + 1)V_o^* \\ I_{r1} = \dfrac{\pi V_o^*}{2L_n Z_r} \end{cases} \tag{2.4}$$

The iterative formulas of Condition II is as (2.5), as shown at the bottom of the page, and (2.6), as shown at the bottom of the page.

Because Condition II is similar to Condition I and $T_d \approx 1$, the initial value under Condition II can be obtained as (2.7), as shown at the bottom of the page.

The iterative formulas of Condition III can be expressed by (2.8), as shown at the bottom of the next page, and (2.9), as shown at the bottom of the next page.

Under Condition III, there is no approximate value for T_n and T_k. However, the initial value under Condition I can still be used, which is verified by the follow-up simulations. The initial value under Condition III is shown as follows.

$$\begin{cases} T_{n(0)} = 1 + \dfrac{4L_n}{\pi^2}(1 - \dfrac{V_i}{V_o^*}) \\ T_{k(0)} = T_{n(0)} \end{cases} \tag{2.10}$$

Since T_k is not used in (2.8), the initial values of the three working conditions can be unified, namely, (2.7) can be the initial value for all three working conditions. In the basic idea of iterative algorithm, the identification of working condition

$$\begin{cases} I_{r0(i+1)} = \dfrac{\pi\left(T_{k(i)}\left(\pi^2 T_{k(i)}\left(T_{n(i)} - T_{k(i)}\right) - 4\right)V_o^* - 4L_n\left(T_{k(i)}V_o^* + \left(T_{n(i)} - T_{k(i)}\right)V_i\right) + 2L_n\pi\left(T_{n(i)} - T_{k(i)}\right)T_{n(i)}I_o^* Z_r\right)}{2L_n\left(4 + 4L_n - \pi^2 T_{k(i)}\left(T_{n(i)} - T_{k(i)}\right)\right)Z_r} \\ I_{r1(i+1)} = \dfrac{-\pi\left(T_{k(i)}\left(\pi^2 T_{k(i)}\left(T_{n(i)} - T_{k(i)}\right) - 4\right)V_o^* - 4L_n\left(T_{k(i)}V_o^* - \left(T_{n(i)} - T_{k(i)}\right)V_i\right) - 2L_n\pi\left(T_{n(i)} - T_{k(i)}\right)T_{n(i)}I_o^* Z_r\right)}{2L_n\left(4 + 4L_n - \pi^2 T_{k(i)}\left(T_{n(i)} - T_{k(i)}\right)\right)Z_r} \\ V_{c0(i+1)} = V_i - V_o^* + \dfrac{1}{4}\pi\left(2I_{r0(i+1)} - 3I_{r0(i+1)}T_{k(i)} - I_{r1(i+1)}T_{k(i)} - 2I_o^* T_{n(i)}\right)Z_r \\ V_{c1(i+1)} = V_i - V_o^* + \dfrac{1}{4}\pi\left(2I_{r0(i+1)} - I_{r0(i+1)}T_{k(i)} + I_{r1(i+1)}T_{k(i)} + 2I_o^* T_{n(i)}\right)Z_r \end{cases} \tag{2.1}$$

$$\begin{cases} T_{k(i+1)} = 1 + \dfrac{\left(I_{r1(i)} + I_{r0(i)}\right)Z_r}{\pi\left(V_{c0(i)} - V_i + V_o^*\right)} \\ T_{n(i+1)} = T_{k(i+1)} + \dfrac{2L_n}{\pi^2 T_{k(i+1)}V_o^*}(\pi(T_{k(i+1)} - 1)I_{r0(i)}Z_r + 2(V_o^* - V_i)) \end{cases} \tag{2.2}$$

$$\begin{cases} I_{r0(i+1)} = \pi(\dfrac{1}{2} - T_{k(i)})\dfrac{V_o^*}{L_n Z_r} \\ V_{c1(i+1)} = \pi T_{n(i)}I_o^* Z_r + \dfrac{\pi^2}{2L_n}T_{k(i)}(1 - T_{k(i)})V_o^* + V_{c0} \\ V_{c2(i+1)} = \dfrac{(I_{r0(i+1)}^2 - I_{r1}^2)(L_n + 1)Z_r^2 + (V_{c0} - V_{c1(i+1)})(V_{c0} + V_{c1(i+1)} - 2V_i)}{4V_i} \\ I_{r2(i+1)} = \sqrt{\dfrac{(V_{c1(i+1)} - V_{c2(i+1)})(V_{c1(i+1)} + V_{c2(i+1)} - 2V_i)}{(L_n + 1)Z_r^2} + I_{r1}^2} \end{cases} \tag{2.5}$$

$$\begin{cases} T_{k(i+1)} = \dfrac{2}{3} + \dfrac{1}{3}\sqrt{\dfrac{6T_{n(i)}L_n I_o^* Z_r}{\pi V_o^*} + 1 - \dfrac{12}{\pi^2}} \\ T_{n(i+1)} = \dfrac{2(V_{c0(i)} + V_{c2(i)})}{\pi(I_{r0(i)} - I_{r2(i)})Z_r} - \dfrac{2(V_{c1(i)} - V_{c2(i)})}{\pi(I_{r1(i)} + I_{r2(i)})Z_r} + T_{k(i+1)} \\ T_{d(i+1)} = 1 - \dfrac{2(V_{c0(i)} + V_{c2(i)})}{\pi T_{n(i+1)}(I_{r0(i)} - I_{r2(i)})Z_r} \end{cases} \tag{2.6}$$

$$\begin{cases} T_{k(0)} = 1 \\ T_{d(0)} = 1 \\ T_{n(0)} = 1 + \dfrac{4L_n}{\pi^2}(1 - \dfrac{V_i}{V_o^*}) \end{cases} \tag{2.7}$$

is added to form a complete iterative algorithm. Under Condition I and Condition II, $V_o^* > V_i$; Under Condition III, $V_o^* < V_i$. The relationship between V_i and V_o^* can be used to distinguish the first two conditions and the third condition. V_{c0} under Condition II is the fixed value, but V_{c0} under Condition I is less than this fixed value. So V_{c0} can be used to distinguish Condition I and Condition II.

With V_i, V_o^*, I_o^*, Z_r and L_n as input and T_n, T_k, T_d, V_{c0}, V_{c1}, V_{c2}, I_{r0}, I_{r1} and I_{r2} as output, the iterative calculation model is shown in Fig. 7.

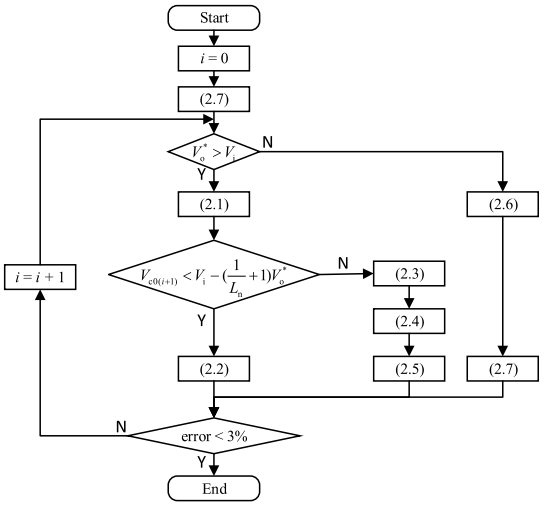

FIGURE 7. The flow chart of iterative algorithm.

Where the error is expressed as follows:

$$\text{error} = \frac{\left|T_{n(i+1)} - T_{n(i)}\right|}{T_{n(i)}} \times 100\% \tag{2.11}$$

All variables influence each other in the iteration process. When the error of T_n is small enough, the error of other variables will also be small.

Take the Condition I as an example: V_i, V_o^*, I_o^*, Z_r and L_n are taken as the input of the iterative calculation model and T_n, T_k, V_{c0}, V_{c1}, I_{r0} and I_{r1} are obtained.

Then the complete time-domain function are obtained as follow, which can be used to draw all waveform.

$t \in (0, \frac{T_k T_r}{2})$:

$$\begin{cases} v_c(t) = I_{r0} Z_r \sin(\omega_r t) + (V_{c0} - V_i + V_o^*)\cos(\omega_r t) \\ \qquad\qquad + V_i - V_o^* \\ i_r(t) = I_{r0}\cos(\omega_r t) - \dfrac{V_{c0} - V_i + V_o^*}{Z_r}\sin(\omega_r t) \\ i_m(t) = I_{r0} + \dfrac{V_o^*}{L_m} t \end{cases} \tag{2.12}$$

$t \in (\frac{T_k T_r}{2}, \frac{T_n T_r}{2})$:

$$\begin{cases} v_c(t) = I_{r1}\sqrt{(L_n+1)} Z_r \sin(\omega_m t - \omega_m \dfrac{T_k T_r}{2}) \\ \qquad\qquad + (V_{c1} - V_i)\cos(\omega_m t - \omega_m \dfrac{T_k T_r}{2}) + V_i \\ i_r(t) = I_{r1}\cos(\omega_m t - \omega_m \dfrac{T_k T_r}{2}) \\ \qquad\qquad - \dfrac{V_{c1} - V_i}{\sqrt{(L_n+1)} Z_r}\sin(\omega_m t - \omega_m \dfrac{T_k T_r}{2}) \\ i_m(t) = i_r(t) \end{cases} \tag{2.13}$$

It is noted from the waveform characteristics of the Condition I and the complete time domain functions that synchronous rectification can be easily achieved.

Based on the complete time-domain function, the peak resonant current I_{rp} and the peak magnetizing current I_{rm} can be both obtained very easily as follow. The two values can be used to design the resonant inductor and the transformer.

$$I_{rp} = \max\left(\sqrt{I_{r0}^2 + \left(\frac{V_{c0} - V_i + V_o^*}{Z_r}\right)^2}, -I_{r0}\right) \tag{2.14}$$

$$I_{mp} = \max(I_{r1}, -I_{r0}) \tag{2.15}$$

$$\begin{cases} I_{r0(i+1)} = -\dfrac{T_{n(i)} V_o^*}{\dfrac{2}{\pi} L_n Z_r} \\ V_{c0(i+1)} = -\dfrac{2}{\pi} T_{n(i)} I_o^* Z_r \\ V_{c1(i+1)} = -\dfrac{V_o^*}{V_i} V_{c0(i+1)} \\ I_{r1(i+1)} = \dfrac{1}{Z_r}\sqrt{\left(V_{c0(i+1)} - V_{c1(i+1)}\right)\left(V_{c0(i+1)} + V_{c1(i+1)} - 2V_i + 2V_o^*\right) + I_{r0(i+1)}^2 Z_r^2} \end{cases} \tag{2.8}$$

$$\begin{cases} X_{(i+1)} = \dfrac{\left(V_{c1(i)} - V_i + V_o^*\right) I_{r0(i)} Z_r - \left(V_{c0(i)} - V_i + V_o^*\right) I_{r1(i)} Z_r}{I_{r0(i)} I_{r1(i)} Z_r^2 + \left(V_{c1(i)} - V_i + V_o^*\right)\left(V_{c0(i)} - V_i + V_o^*\right)} \\ T_{k(i+1)} = 1 + \dfrac{1}{\pi}\left(\sqrt[3]{\dfrac{3X_{(i+1)}}{2} + \sqrt{\dfrac{9X_{(i+1)}^2}{4} + 1}} + \sqrt[3]{\dfrac{3X_{(i+1)}}{2} - \sqrt{\dfrac{9X_{(i+1)}^2}{4} + 1}}\right) \\ T_{n(i+1)} = \dfrac{2(V_{c1(i)} + V_{c0(i)})}{\pi(I_{r0(i)} - I_{r1(i)})Z_r} + T_{k(i+1)} \end{cases} \tag{2.9}$$

Similar to the calculation for I_{rp} and I_{rm}, the loss expression can be easily obtained based on the complete time-domain function. But the loss expression of algebraic is complex and is not the focus of this paper. Thus, the specific expressions about the loss will not be presented here.

IV. VERIFICATION

In order to demonstrate the advantages of the methods proposed in this paper, the comparison will be made from global and local perspective.

From the global perspective, voltage gain is the most concerned design requirements of LLC converter, and is also the frequently analyzed object in FHA method. Besides, when the demand of maximum voltage gain under heavy load is satisfied, the demand of maximum voltage gain under light load will also be satisfied. Therefore, the curve of voltage gain under heavy load is regarded as the key comparison objective from a global perspective.

From the local perspective, in some specific working condition, the magnetic component design, loss analysis and synchronous rectification analysis will be more accurate with a more accurate waveform. The waveform can be deduced by time-domain function with the key variables V_i, V_o^*, I_o^*, Z_r, L_n, T_n, T_k, T_d, V_{c0}, V_{c1}, V_{c2}, I_{r0}, I_{r1} and I_{r2} involved. Therefore, these key variables are regarded as the key comparison objectives from the local perspective. At the same time, the deduced waveform is compared with the real waveform. These above comparisons are carried out under three typical working conditions including Condition I, Condition II and Condition III.

In order to demonstrate the simplicity of iterative calculation, the calculation cost of iterative calculation is analyzed.

The relevant parameters of LLC resonant converter used in the experimental verification are shown in the table below.

TABLE 2. Related parameters of LLC resonant converter.

Symbols	Parameter names	Value
V_i	Input voltage	100 V
L_r	Resonant inductor	28.8 μH
C_r	Resonant capacitor	23.5 nF
L_m	Excitation inductance	100 μH
f_r	Resonant frequency	193.46 kHz
N	Turn ratio of transformer	410/48
$R_{ds(on)}$	On-resistance of diodes	1.7 mΩ
V_d	Conductance Voltage of diodes	0.8 V

Considering the influence of diodes' on-resistance and conductance voltage, V_o is modified in iterative calculation and fundamental harmonic analysis.

A. VOLTAGE GAIN CURVE COMPARISON

The voltage gain curve of LLC resonant converter determines the voltage conversion range of the converter, which is of great significance to the design of the converter.

The fundamental harmonic analysis method has simple calculation and low accuracy while the simulation based on Simulink has complex calculation and high accuracy. Compared with the fundamental harmonic analysis method and the simulation, the simplicity and the accuracy of the iterative calculation model can be presented. Compared with experimental results, the accuracy of the iterative calculation model can be further proved.

1.35 Ω load resistance is taken as the heavy load condition, the switch frequency changes at the range of 130-250 kHz, and the output voltage curves are compared with the switching frequency under the fundamental harmonic analysis method (I), simulation results (II), experimental results (III) and the method proposed in this paper (IV).

For calculation simplicity, the iterative times of the model is less than 10, which means the calculation is less than the simulation method.

For calculation accuracy, it can be seen from Fig. 8 that the fundamental analysis method is close to the simulation and experiment when the switching frequency is close to the resonance frequency, but when the switching frequency is far away from the resonance frequency, the error becomes larger and larger. In contrast, the curve of the iterative calculation method is basically consistent with the curve of simulation and experiment, the accuracy is very high, and the error will not increase when the difference between the switching frequency and resonant frequency increase.

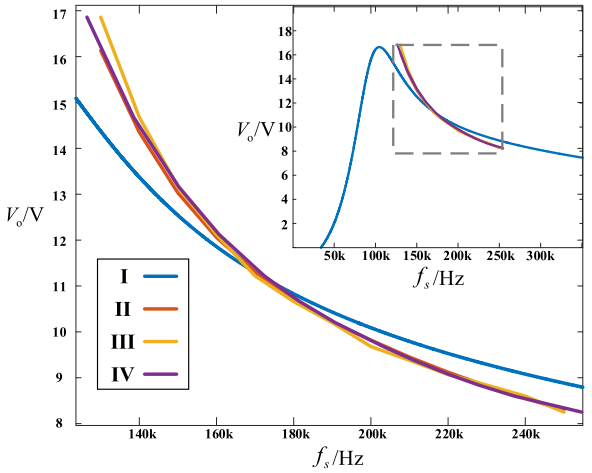

FIGURE 8. Comparison of output voltage curve with switch frequency.

B. KEY VARIABLES COMPARISON

On the basis of above analysis, the corresponding points of the three conditions (Condition I: $f_s = 160$ kHz and $R = 1.35\Omega$; Condition II: $f_s = 160$ kHz and $R = 2.7\Omega$; Condition III: $f_s = 220$ kHz and $R = 1.35\Omega$) are selected for further experiments, and the variables of iterative calculation are compared with simulation and experiment. Tektronix p2200 probes and Cybertek CPL8100B probes are used to measure the voltage of the resonant capacitor and the current of the resonant inductor. And the simulation results are based on the Simulink.

It can be seen from the comparison table of key variables that the calculation results based on the method proposed in

TABLE 3. Comparison of key variables.

Key Variables	Experiment	Calculation	Simulation
	Condition I		
f_s / kHz	160	161.25	160
V_o / V	12.12	12.06	12.06
V_{c0} / V	–88	–82	–82
V_{c1} / V	72	51	50
I_{r0} / A	–1.7	–1.61	–1.60
I_{r1} / A	1.5	1.49	1.47
T_k	1.153	1.022	1.019
	Condition II		
f_s / kHz	160	161.56	160
V_o / V	12.26	12.31	12.31
V_{c0} / V	–66	–52	–52
V_{c1} / V	28	17	16
V_{c2} / V	46	42	41
I_{r0} / A	–1.1	–1.54	–1.53
I_{r1} / A	1.4	1.53	1.52
I_{r2} / A	1.6	1.71	1.72
T_k	0.991	1.002	1.003
T_d	0.882	0.952	0.945
	Condition III		
f_s / kHz	220	218.71	220
V_o / V	9.12	9.12	9.12
V_{c0} / V	–46	–38	–38
V_{c1} / V	41	35	35
I_{r0} / A	–0.6	–1.04	–1.05
I_{r1} / A	1.4	1.51	1.49
T_k	0.814	0.862	0.856

this paper are the same as the simulation results under ideal conditions and the relative errors are less than 3%. But the error between the calculation results and the experimental results is large. Both simulation and calculation models are based on ideal models, so the calculation model and theoretical analysis are consistent under ideal conditions. The main differences between the experiment and ideal condition are practical stray and parasitics, which cause such large error. The switching frequency used in the experiment is low, so the inductance parameters are large and the influence of the practical stray or parasitics is small. When the switching frequency increases, the influence of the practical stray or parasitics cannot be ignored. Therefore, the influence need to be analyzed to correct the related parameters in the iterative calculation model, which does not change the model and its accuracy.

The calculation waveforms of Fig. 9 are drawn according to the time-domain function expression by using the results of the iterative model. For example, Fig. 9(a) is drawn according to (2.12) and (2.13). The simulation waveform is basically the same as the calculated waveform. Here, only the difference between the calculated waveform and the actual waveform is compared.

It can be seen from Fig. 9 that although there are some errors due to practical stray and parasitics, the calculated waveform is very similar to the experimental waveform. And

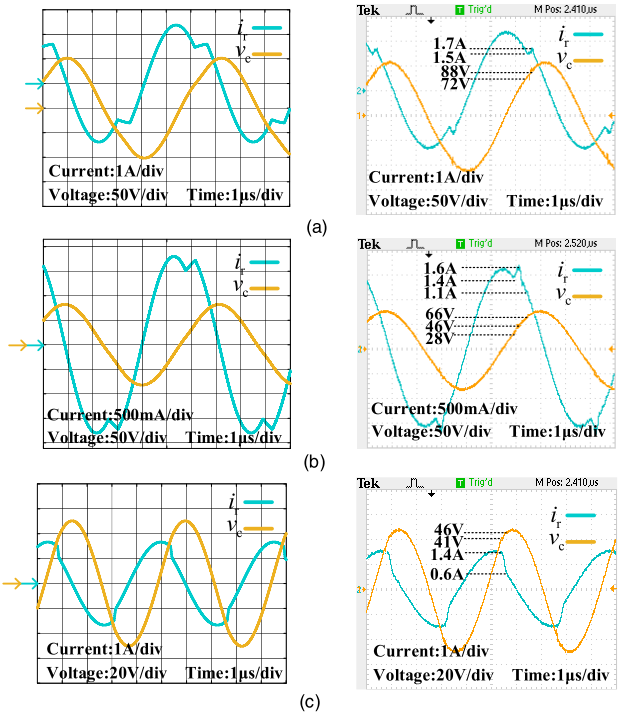

FIGURE 9. Comparison of calculation (left) and experiment (right) waveforms under: (a) f_s = 160 kHz and R = 1.35 Ω; (b) f_s = 160 kHz and R = 2.7 Ω; (c) f_s = 220 kHz and R = 1.35 Ω.

the accuracy of the method proposed in this paper can meet the requirements of the design phase for LLC converters.

C. SIMPLICITY OF ITERATIVE CALCULATION

By analyzing the iterative model, the following table about the calculation cost for each iteration step can be obtained. See Appendix D for detailed analysis.

TABLE 4. The calculation cost for each iteration step.

	Condition I	Condition II	Condition III
Additions	23	22	16
Multiplications	27	19	23
Divisions	3	6	2
Extractions of a root	0	2	4

10 or less iterations are spent in the previous comparison experiments. Compared with non-linear solution software, the calculation cost of our proposed model are much fewer. That means the proposed model has the capability to be embedded into the DSP or other processors to be run in real-time with few resource occupation.

V. CONCLUSION

Based on suitable assumption and simplification, the time-domain equations are simplified by using the voltage, current and time of the switching points as variables. The simplified time-domain equations under three conditions are obtained, and an effective iterative model is designed to solve the

relevant variables of the switching points without sophisticated nonlinear solution software. From a global perspective, the method in this paper can obtain a voltage gain curve with high accuracy in a relatively wide frequency range. From a local perspective, the relative errors between the calculated results and the simulation results are less than 3%. The relative errors between the calculation and the experiment is a little large because of practical stray and parasitics which will be added to the simplified equations to further improve accuracy in the future. And more model-based analysis about the loss, the design of the magnetic components, and the synchronous rectification will be done in the future. Besides, the calculation of iterative model is very less and can be realized on DSP or other processors in real-time.

REFERENCES

[1] C. Fei, F. C. Lee, and Q. Li, "High-efficiency high-power-density LLC converter with an integrated planar matrix transformer for high-output current applications," *IEEE Trans. Ind. Electron.*, vol. 64, no. 11, pp. 9072–9082, Nov. 2017.

[2] M. Mu and F. C. Lee, "Design and optimization of a 380–12 V high-frequency, high-current LLC converter with GaN devices and planar matrix transformers," *IEEE J. Emerg. Sel. Topics Power Electron.*, vol. 4, no. 3, pp. 854–862, Sep. 2016.

[3] W. Zhang, Z. Xu, Z. Zhang, F. Wang, L. M. Tolbert, and B. J. Blalock, "Evaluation of 600 V cascode GaN HEMT in device characterization and all-GaN-based LLC resonant converter," in *Proc. IEEE Energy Convers. Congr. Expo.*, Sep. 2013, pp. 3571–3578.

[4] M. H. Ahmed, M. A. de Rooij, and J. Wang, "High-power density, 900-W LLC converters for servers using GaN FETs: Toward greater efficiency and power density in 48 V to 612 V converters," *IEEE Power Electron. Mag.*, vol. 6, no. 1, pp. 40–47, Mar. 2019.

[5] Z. Zhao, Q. Xu, Y. Dai, and A. Luo, "Minimum resonant capacitor design of high-power LLC resonant converter for comprehensive efficiency improvement in battery charging application," *IET Power Electron.*, vol. 11, no. 11, pp. 1866–1874, Sep. 2018.

[6] H. Wang, Y. Chen, Y.-F. Liu, J. Afsharian, and Z. Yang, "A passive current sharing method with common inductor multiphase LLC resonant converter," *IEEE Trans. Power Electron.*, vol. 32, no. 9, pp. 6994–7010, Sep. 2017.

[7] H. Huang, "FHA-based voltage gain function with harmonic compensation for LLC resonant converter," in *Proc. 25th Annu. IEEE Appl. Power Electron. Conf. Expo. (APEC)*, Feb. 2010, pp. 1770–1777.

[8] X. Xie, J. Zhang, C. Zhao, Z. Zhao, and Z. Qian, "Analysis and optimization of LLC resonant converter with a novel over-current protection circuit," *IEEE Trans. Power Electron.*, vol. 22, no. 2, pp. 435–443, Mar. 2007.

[9] G. Ivensky, S. Bronshtein, and A. Abramovitz, "Approximate analysis of resonant LLC DC-DC converter," *IEEE Trans. Power Electron.*, vol. 26, no. 11, pp. 3274–3284, Nov. 2011.

[10] J. Liu, J. Zhang, T. Q. Zheng, and J. Yang, "A modified gain model and the corresponding design method for an LLC resonant converter," *IEEE Trans. Power Electron.*, vol. 32, no. 9, pp. 6716–6727, Sep. 2017.

[11] Z. Hu, L. Wang, H. Wang, Y.-F. Liu, and P. C. Sen, "An accurate design algorithm for LLC resonant converters—Part I," *IEEE Trans. Power Electron.*, vol. 31, no. 8, pp. 5435–5447, Aug. 2016.

[12] Z. Hu, L. Wang, Y. Qiu, Y.-F. Liu, and P. C. Sen, "An accurate design algorithm for LLC resonant converters—Part II," *IEEE Trans. Power Electron.*, vol. 31, no. 8, pp. 5448–5460, Aug. 2016.

[13] A. K. Singh, P. Das, and S. K. Panda, "Analysis and design of SQR-based high-voltage LLC resonant DC–DC converter," *IEEE Trans. Power Electron.*, vol. 32, no. 6, pp. 4466–4481, Jun. 2017.

[14] M. Mohammadi and M. Ordonez, "LLC synchronous rectification using homopolarity cycle modulation," in *Proc. IEEE Energy Convers. Congr. Expo. (ECCE)*, Oct. 2017, pp. 3776–3780.

[15] M. Mohammadi and M. Ordonez, "Synchronous rectification of LLC resonant converters using homopolarity cycle modulation," *IEEE Trans. Ind. Electron.*, vol. 66, no. 3, pp. 1781–1790, Mar. 2019.

[16] M. Mohammadi, F. Degioanni, M. Mahdavi, and M. Ordonez, "Small-signal modeling of LLC converters using homopolarity cycle," *IEEE Trans. Power Electron.*, vol. 35, no. 4, pp. 4076–4093, Apr. 2020.

[17] E. S. Glitz and M. Ordonez, "MOSFET power loss estimation in LLC resonant converters: Time interval analysis," *IEEE Trans. Power Electron.*, vol. 34, no. 12, pp. 11964–11980, Dec. 2019.

[18] E. S. Glitz, J.-D. Hsu, and M. Ordonez, "Power loss estimation in LLC synchronous rectification using rectifier current equations," *IEEE Trans. Ind. Electron.*, vol. 67, no. 5, pp. 3696–3704, May 2020.

[19] H. Xu, Z. Yin, Y. Zhao, and Y. Huang, "Accurate design of high-efficiency LLC resonant converter with wide output voltage," *IEEE Access*, vol. 5, pp. 26653–26665, 2017.

[20] A. Awasthi, S. Bagawade, A. Kumar, and P. Jain, "An exact time domain analysis of DCM boost mode LLC resonant converter for PV applications," in *Proc. IECON-44th Annu. Conf. IEEE Ind. Electron. Soc.*, Oct. 2018, pp. 1005–1010.

[21] S. Karimi and F. Tahami, "A comprehensive time-domain-based optimization of a high-frequency LLC-based li-ion battery charger," in *Proc. 10th Int. Power Electron., Drive Syst. Technol. Conf. (PEDSTC)*, Feb. 2019, pp. 415–420.

[22] W. Feng, F. C. Lee, and P. Mattavelli, "A hybrid strategy with simplified optimal trajectory control for LLC resonant converters," in *Proc. 27th Annu. IEEE Appl. Power Electron. Conf. Expo. (APEC)*, Feb. 2012, pp. 1096–1103.

JINGKAI NIU (Graduate Student Member, IEEE) was born in Shanxi, China, in 1993. He received the B.Sc. degree from Beijing Jiaotong University, Beijing, China, in 2016, where he is currently pursuing the Ph.D. degree in electrical engineering with the School of Electrical Engineering. His current research interests include resonant converters and application of wide band gap semiconductor devices.

YIBING TONG received the M.S. degree from Northern Jiaotong University, Beijing, China, in 1998. He has been an Associate Professor with the School of Electrical Engineering, Beijing Jiaotong University, since 1998. His general research interests include new energy generation technologies and microgrid technology.

QING DING was born in Hubei, China, in 1982. He is currently a Doctor and a Senior Engineer with Shenzhen Power Supply Company Ltd., China. His research interests include new energy and electromagnetic environment.

XUEZHI WU received the B.S. degree in application of electronic technology and the M.S. degree in power electronics and power drives from Beijing Jiaotong University, Beijing, China, in 1996 and 1999, respectively, and the Ph.D. degree in power electronics and power drives from Tsinghua University, Beijing, in 2002. His general research interests include new energy grid connection technology, microgrid converter, microgrid systems, and high-power motor control technology.

XIAOMIN XIN was born in Inner Mongolia, China, in 1995. He received the bachelor's degree in electrical engineering from Beijing Jiaotong University, in 2018, where he is currently pursuing the master's degree. His research interests include high-frequency LLC topology and its applications.

XIN WANG was born in Henan, China, in 1995. He received the bachelor's degree in engineering from Beijing Jiaotong University, in 2018, where he is currently pursuing the master's degree. His research interests include power electronics and power transmission.